NASA TECHNICAL NOTE

$c.1$

EXPERIMENTAL INVESTIGATION OF NUCLEATE BOILING BUBBLE DYNAMICS IN NORMAL AND ZERO GRAVITIES

*by Thomas H. Cochran, John C. Aydelott,
and Charles M. Spuckler*

*Lewis Research Center
Cleveland, Ohio*

NATIONAL AERONAUTICS AND SPACE ADMINISTRATION • WASHINGTON, D. C. • FEBRUARY 1968

EXPERIMENTAL INVESTIGATION OF NUCLEATE BOILING

BUBBLE DYNAMICS IN NORMAL AND ZERO GRAVITIES

By Thomas H. Cochran, John C. Aydelott,
and Charles M. Spuckler

Lewis Research Center
Cleveland, Ohio

NATIONAL AERONAUTICS AND SPACE ADMINISTRATION

EXPERIMENTAL INVESTIGATION OF NUCLEATE BOILING
BUBBLE DYNAMICS IN NORMAL AND ZERO GRAVITIES

by Thomas H. Cochran, John C. Aydelott,
and Charles M. Spuckler

Lewis Research Center

SUMMARY

The effects of gravity on the dynamics of bubbles generated on a flat horizontal sur-
face are investigated in the heat-flux range defined as the discrete bubble region over a
range of subcoolings, fluid properties, and heat-transfer rates. The zero-gravity data
were obtained by allowing the experiment package to free fall in a 2.2-second drop tower,
which permitted the attainment of less than 10^{-5} times Earth gravity. Data taken from
high-speed motion pictures indicated that boiling was independent of gravity at high sub-
cooling and that the transition from the discrete bubble region occurred at a lower heat
flux in zero gravity than in normal gravity. Application of an analysis to the data indi-
cated that a newly defined pressure force was of importance in bringing about bubble
separation.

INTRODUCTION

The space exploration program of the NASA is heavily dependent on the use of liquid
hydrogen as a rocket fuel. Hydrogen has been very attractive either for use as a pro-
pellant, because of the high specific impulse it produces when reacted with an oxidizer,
or for use as a heated expellant as in a nuclear rocket.

The low equilibrium temperature of liquid hydrogen makes it difficult to insulate a
storage tank sufficiently to prevent a net heat gain. Under these conditions, the tank
pressure will increase and the liquid bulk may become subcooled (ref. 1). Attempts to
calculate the rate of pressure rise have not been successful because of a lack of know-

ledge of the various heat-transfer mechanisms involved. Consequently, one of the areas of interest for both normal- and reduced-gravity research has been heat transfer and, in particular, the subcooled nucleate boiling process.

The pioneering work in this field was performed by Siegel and coworkers (refs. 2 to 6) at the Lewis Research Center. In this work a $12\frac{1}{2}$-foot (3.82-m) drop tower was used, which made available approximately 1 second of reduced-gravity time. Thus, photographs could be taken that showed the gravitational effect on water boiling at saturation conditions. This work revealed the importance of bubble dynamics on heat-transfer processes in low-gravity environments.

An extension of this initial work, performed by the authors, was a study of the effect of zero gravity on boiling in the discrete bubble region for a range of subcoolings (0° to 40° F; 0° to 22.22° K) (ref. 7) and various fluid properties (surface tension and viscosity) (ref. 8). Included was a study of the dynamics of a generated bubble, which resulted in a new approach to the formulation of the buoyancy force, and the definition of a force associated with the unbalanced pressure across the top surface of the bubble. Analysis of photographic data included a statistical study of the maximum radii and lifetimes of the generated bubbles and calculation of the forces acting during the growth and collapse of the bubbles on the generating surface.

The objectives of this report are as follows:

(1) To present the results of a further study of the effect of gravity on boiling at various heat-transfer rates in the discrete bubble region with a 10-percent-by-volume ethanol-water solution

(2) To summarize the work of the authors to date concerning the effect of gravity on boiling bubble dynamics

SYMBOLS

D	diameter, ft; m
F	force, lb force; N
F_B	buoyancy force, lb force; N
F_{dr}	drag force, lb force; N
F_{dy}	dynamic force, lb force; N
F_p	pressure force, lb force; N
F_s	total surface-tension force, lb force; N
F_{sy}	surface-tension force, lb force; N

g   acceleration due to gravity, ft/sec^2; m/sec^2

g_c gravitational constant, (lb mass/lb force)(ft/sec^2); (kg/N)(m/sec^2)

M   mass

R   radius measured from bubble center of mass, ft; m

R_t radius of curvature of top surface, ft; m

T   temperature, $^\circ$F; $^\circ$K

t   time, sec

V   bubble total volume, ft^3; m^3

v_b bubble volume directly over base, ft^3; m^3

v   velocity, ft/sec; m/sec

Y   distance above heater surface to bubble center of mass, ft; m

μ dynamic viscosity, (lb force)(sec)/ft^2; (N)(sec)/m^2

ρ density, lb mass/ft^3; kg/m^3

σ surface tension, lb force/ft; N/m

τ dimensionless time

φ contact angle

Subscripts:

b   base

l liquid

max   maximum

S   heater surface

sat   saturated conditions

v   vapor

ANALYSIS

Bubble Model

The heat-flux range in which the experiments where conducted is referred to as the discrete bubble region. In such a range in normal gravity, the bubbles generally grow undistrubed on the heated surface, and the heat-transfer mechanism is highly dependent

on the disturbance in the liquid caused by the growth and departure of the bubbles. Therefore, a knowledge of the motion and growth characteristics of individual bubbles is basic to a complete understanding of the phenomenon. A model is assumed in order to describe the motion of a bubble. The only restrictions placed on the model are that it be symmetric with respect to the y-axis, as shown in figure 1, and that the surface of the bubble directly over the base be a spherical segment.
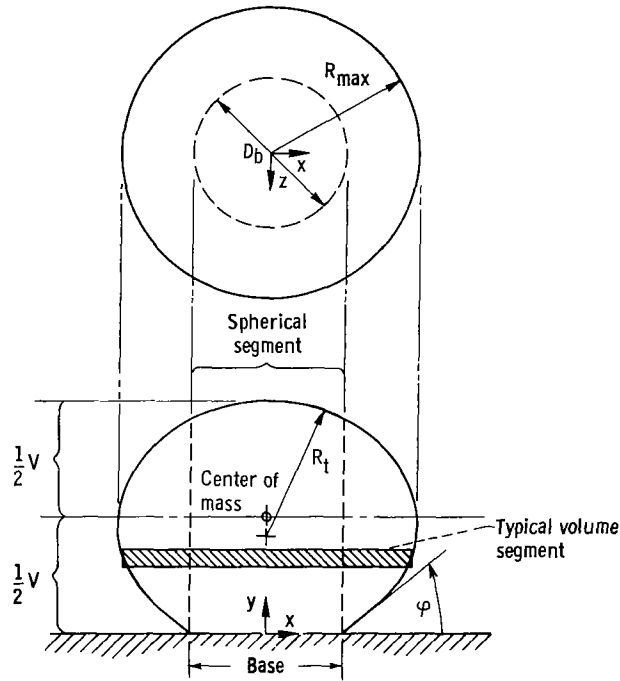

Figure 1. - Bubble model.

Simple geometric formulas cannot be used to calculate bubble total volume because of the general nature of the model. Consequently, volume is determined by an integrative method in which a bubble is divided into segments, the volumes of which can be approximated if they are assumed to be circular disks. The sum of the volumes of the disks produces the total volume. The volume directly over the bubble base is obtained by assuming that it is a right circular cylinder with a segment of a sphere as a cap.

The center of mass of the bubble is used to describe its motion. If uniform density is assumed, the center of mass is approximated from the location of the plane parallel to the heater surface which divides the bubble in half with respect to its total volume.

Bubble Forces

General. - An analytical investigation of the dynamics of a bubble on a heated sur-

face results in the identification of buoyancy, surface-tension, pressure, drag, and dynamic forces. A force due to the vapor weight should also be included for all fluids near the critical thermodynamic state and for some fluids that do not have a large difference between liquid and vapor density, such as hydrogen. However, for the experimental conditions under consideration, this force may be neglected.

Buoyancy force. - Buoyancy on an object submerged in a liquid is caused by the difference between the external hydrostatic pressure force on its top surface and the external hydrostatic pressure force on its bottom surface. Therefore, for a bubble attached to a heated surface, the volume of the bubble directly over the base does not generate a buoyant force because of the lack of liquid beneath the base; therefore, the buoyancy force, as derived in reference 7, is

$$F_B = (V - V_b)\rho_l \frac{g}{g_c} \tag{1}$$

and it acts in a direction opposite to the acceleration due to gravity.

Surface-tension force. - A surface-tension force is generated at the boundary of a liquid and some other substance, such as a vapor or a solid. Therefore, such a force exists at the base of a bubble attached to the heater surface at the boundary of the liquid, vapor, and solid surfaces. The direction of this force is perpendicular to the boundary and in the plane of the liquid-vapor interface. Surface tension is defined as the ratio of the surface force to the length along which the force acts, which, for an attached bubble, is

$$\sigma_S = \frac{F_s}{\pi D_b} \tag{2}$$

The vertical component of this force acts to retard the movement of the bubble away from the surface and may be expressed as

$$F_{sy} = \sigma_S \pi D_b \sin \varphi \tag{3}$$

The contact angle φ is the angle at the base between the liquid-vapor interface and the heater surface, as shown in figure 1.

Pressure force. - The net force due to the uniform pressure on a bubble surface is zero for a bubble surrounded by liquid. For a bubble attached to a surface, however, the net internal pressure force on the spherical surface area directly over the base is unbalanced. Because the pressure is greater inside the bubble than outside, the force acts to remove the bubble from the surface. The detailed derivation of this force in reference 7 yields

$$F_p = \frac{1}{2} \frac{\pi D_b^2}{R_t} \sigma_{sat} \tag{4}$$

Drag force. - Viscous effects on a bubble are concerned with the motion of the liquid which surrounds the bubble; therefore, a knowledge of the liquid flow fields is necessary. In reference 7, it was observed that during the growth of a bubble the liquid flow is similar to a source flow. Comparison of the viscous and liquid inertia terms in the equation of motion, as presented in reference 8, indicates that for this flow condition the viscous terms may be neglected.

During collapse of a bubble there was evidence of flow around the liquid-vapor interface. Consequently, the viscous effects in a direction perpendicular to the heater surface may be represented in the form of a drag force,

$$F_{dr} = 12 \mu_l \pi R_{max} \frac{dY}{dt} \tag{5}$$

as derived in reference 7.

Dynamic force. - The last force to be considered is termed the dynamic force F_{dy}. This force is associated with effects on the bubble caused by the dynamics of the bubble and the liquid flow field surrounding the bubble. The nature of this dynamic force has not been clearly defined, so that direct formulation is speculative. Therefore, in this work, the force is obtained by applying Newton's second law of motion to the generated vapor masses, or

$$\sum F = \frac{d}{dt} (M_v v) \tag{6}$$

If it is assumed that the positive force direction is that of increasing y, as shown in figure 1, the left side of equation (6) may be expanded in terms of the identified forces:

$$F_B + F_p - F_{sy} - F_{dr} + F_{dy} = \frac{d}{dt} (M_v v) \tag{7}$$

If, at any instant, a bubble is considered to be a rigid body whose motion is described by the movement of its center of mass, the inertia side of the equation may be expanded in terms of measurable quantities such that

$$F_B + F_p - F_{sy} - F_{dr} + F_{dy} = \frac{\rho_v}{g_c} \left(\frac{dV}{dt} \frac{dY}{dt} + V \frac{d^2Y}{dt^2} \right) + \frac{V}{g_c} \frac{dY}{dt} \frac{d\rho_v}{dt} \tag{8}$$

6

When the bubble is observable on the heater surface, the absolute pressure changes within the bubble are small, so that the change of vapor density with time may be considered negligible. Therefore, when the last term on the right in equation (8) is dropped, the equation solved for the dynamic force becomes

$$F_{dy} = \frac{\rho_v}{g_c}\left(\frac{dV}{dt}\frac{dY}{dt} + V\frac{d^2Y}{dt^2}\right) + F_{dr} + F_{sy} - F_B - F_p \qquad (9)$$

In this approach to the problem, the dynamic force term implicitly contains all the terms necessary to satisfy the equation of motion. Although the method of formulation yields the magnitude of this force, it does not provide explicit information regarding the cause or causes of the force. It is believed that the bulk of this force is associated with the momentum of the liquid surrounding the vapor, or what has been termed the inertia force by other workers in the field.

APPARATUS, EXPERIMENTAL PROCEDURE, AND DATA REDUCTION

The zero-gravity data were obtained in a drop tower (fig. 2) by allowing the experiment package to free fall unguided for 85 feet (25.91 m). A gravity level of less than 10^{-5} times Earth gravity (termed zero gravity in this work) resulted from the package falling in a protective air-drag shield. Deceleration occurred after 2.25 seconds when wooden spikes, mounted to the drag shield, embedded in a box of sand. The experiment package contained a boiling apparatus, camera and lighting equipment, power supplies, and associated controls. Within the boiling apparatus were the primary heater (a Chromel strip with an effective heating length of 0.50 in. (1.27 cm)), a secondary heater which was used to control the temperature of the bulk of the liquid, a thermistor to monitor the bulk temperature, and a temperature-sensing device on the underside of the primary heater. The 16-millimeter motion-picture camera provided a filming rate of approximately 6500 pictures per second.

Prior to a data run, the glassware was cleaned and the primary heater was polished and rinsed with ethanol. The heater surfaces were all polished the same amount with emery paper in an effort to provide each with approximately the same roughness, and hence, approximately the same range of nucleation cavity sizes. The test liquid was deaerated by boiling prior to its insertion in the boiling apparatus. After filling the boiler and raising the package to the top of the drop tower, the test liquid was heated to its approximate saturation temperature with the secondary heater. Power to this heater was removed, and the primary heater was turned on and set at a power level that initia-

Experiment in
predrop position

Deceleration
spikes

Hoist

Assembly
area

Sandbox

Sand storage hopper

Clean and
control rooms

Access
bridge

Elevator

Work area

N

Up   Down
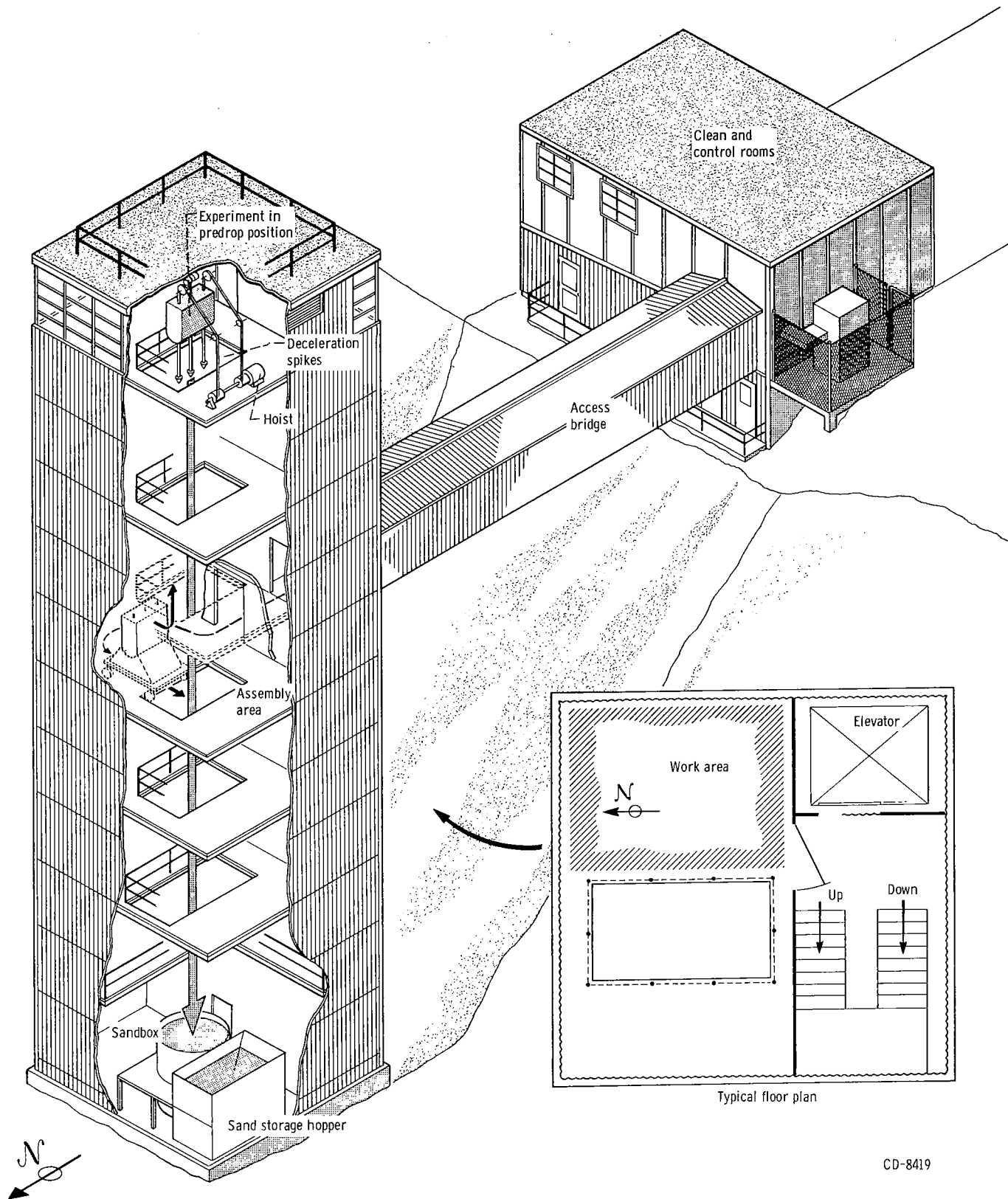
Typical floor plan

N

CD-8419

Figure 2. - 2.2-Second drop tower.

ted boiling. Because the heat input by the strip heater was not sufficient to maintain saturation conditions, the bulk cooled to the desired subcooling. The power level to the primary heater was then increased to the desired level, and the package was dropped. Motion pictures were taken during the last 1.25 seconds of zero-gravity time. Normal-gravity testing was the same as just described with the addition that the temperature-sensing device mounted beneath the primary heater was monitored.

The bubbles recorded on the film were viewed, measured, and counted on a motion analyzer that magnified the image eight times. A statistical analysis involved the recording of bubble lifetime and maximum radius for as many as 15 noncoalescing bubbles at each test condition. Bubbles were selected from as many different sites as possible in order to negate cavity-size effects on the statistical results. For a more detailed description of the previously described equipment and procedures see references 7 and 8.
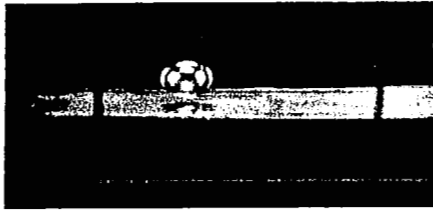
EFFECTS OF HEAT-TRANSFER RATE ON BUBBLE DYNAMICS

The effects of heat-transfer rate were investigated with a 10-percent-by-volume ethanol-water solution. Photographic data showed that, at the higher subcooling tested ($T_{sat} - T_{bulk} \cong 20^O$ F (11.11^O K)), under all test conditions continuous growth bubbles were dominant. (Continuous growth bubbles are those in which volume increases, reaches a maximum, and then decreases until separation from the surface occurs.) However, at the highest heat flux, there did appear to be a slight increase in coalescence in zero gravity as compared to normal gravity.

At the lower subcooling tested ($T_{sat} - T_{bulk} \cong 6^O$ F; 3.34^O K) in normal gravity, there was an increase in coalescence with increased heat flux, but continuous growth bubbles again dominated the phenomenon. Also at low subcooling for the lower heat fluxes, the difference between the zero- and normal-gravity data was a slight increase in coalescence and the presence of a few oscillators (bubbles that alternately grow and collapse) in zero gravity.

A significant difference between the normal- and zero-gravity boiling phenomena was observed at the higher heat fluxes and low subcooling. As shown in figure 3, in zero gravity the relatively high bubble population density, coupled with the fact that the bubbles lingered above the surface after separation, caused a significant increase in coalescence; and the heater strip eventually was obscured. This condition indicates a transition from the discrete bubble region and that the upper limit of the discrete bubble region was lower in zero gravity than in normal gravity.

A statistical study of the behavior of bubble average maximum radii and lifetime as a function of heat-transfer rate is shown in figure 4. No data were obtained either for
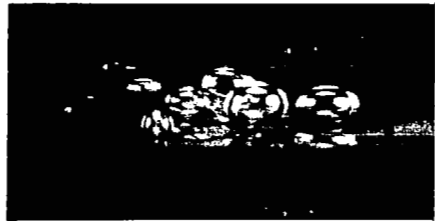
Normal gravity   Zero gravity
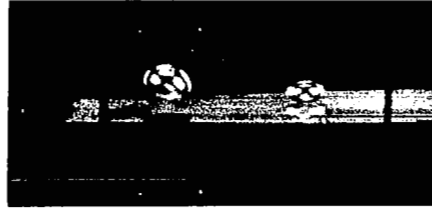
Heat-transfer rate, Btu/(hr)(ft^2); W/m^2:   24 800; 7820

44 000; 13 880

64 900; 20 250

90 000; 28 400

C-67-2605

114 000; 35 950

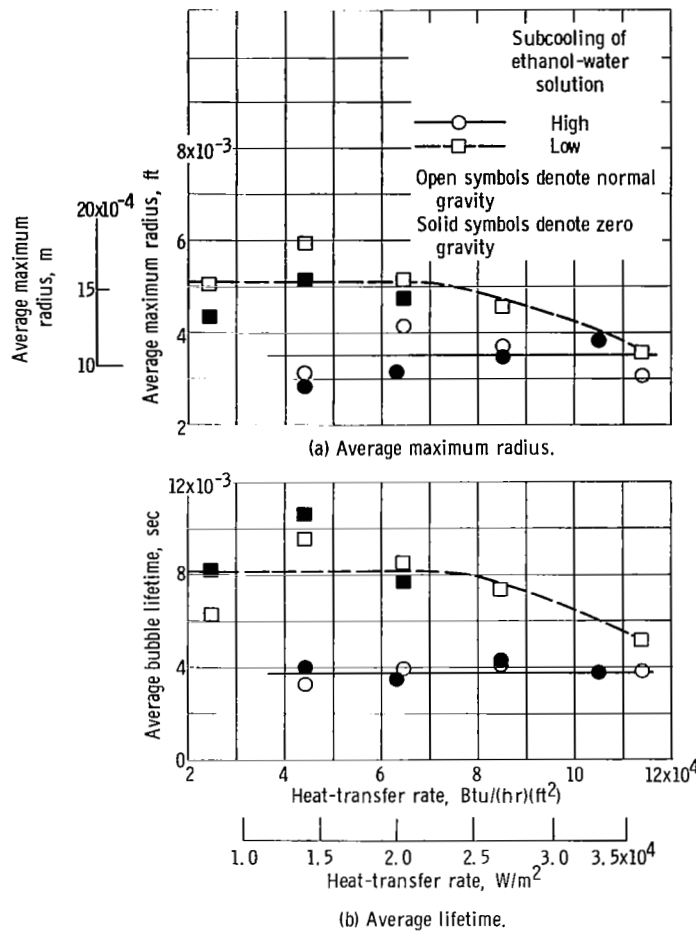Figure 3. - Effect of heat-transfer rate on boiling in normal and zero gravities.

10

Figure 4. - Effects of heat-transfer rate on bubble maximum radius and lifetime in normal and zero gravities.

the lowest heat flux at high subcooling in either normal or zero gravity, because of the lack of nucleation, or for the high heat-transfer rates at low subcooling in zero gravity, because of the aforementioned transition out of the discrete bubble region. At the lower heat fluxes, the separate curves indicate that an increase in subcooling resulted in a decrease in both bubble average maximum radius and lifetime. This corroborates the previous findings of the authors (refs. 7 and 8). It is also apparent from the data that, at lower heat fluxes for lower subcoolings and at all heat fluxes for higher subcoolings, the average maximum-radii and lifetime characteristics of bubbles were independent of heat-transfer rate and gravity. The fact that maximum radii are independent of heat flux for low values in normal gravity has also been reported in reference 9. The normal-gravity, high heat flux, low subcooling data show that a decrease in maximum radii and lifetime occurred. This result may be explained as follows:

11

(1) Bubble average surface-contact area decreased considerably above a heat flux of 60 000 Btu per hour per square foot (18 900 W/m^2), as predicted by Gaertner (ref. 10).

(2) The coalescence of larger bubbles resulted in their exclusion from the statistical sample so that the data are more heavily weighted in favor of the smaller bubbles. Probably a combination of these two causes brought about the noted reduction.

The effect of heat-transfer rate on bubble population density for high and low subcoolings in normal and zero gravities is shown in figure 5. There is no apparent trend
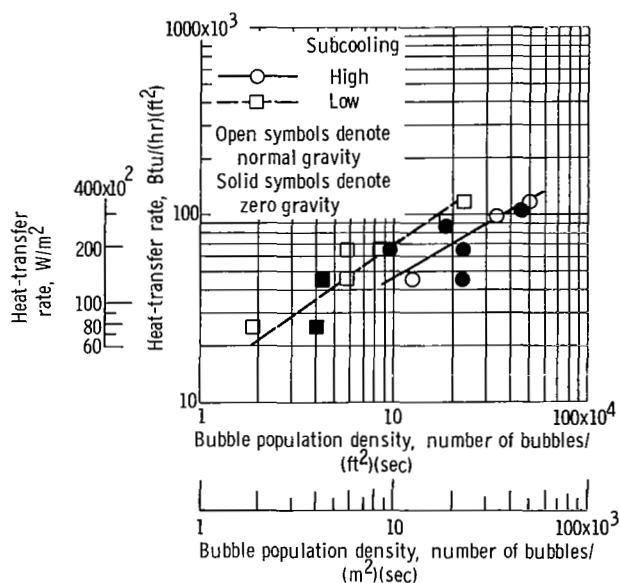

Figure 5. - Effect of heat-transfer rate on bubble population density for high and low subcoolings.

with respect to gravity level, and the change in population density with heat flux is expected from previous findings, such as reference 11. The notable effect was that caused by subcooling, as shown by the separate curves in figure 5. A trend to higher population densities for higher subcoolings at a particular heat flux was also found in the data of reference 7.

A summary of the effects of heat-transfer rate on bubble dynamics is presented in table I.

TABLE I. - EFFECTS OF HEAT FLUX ON BUBBLE CHARACTERISTICS

AS FUNCTION OF GRAVITY LEVEL AND SUBCOOLING

Characteristic	Low subcooling	High subcooling
Type of bubbles	No apparent effect of heat flux. Continuous growth in normal gravity. Continuous growth and a few oscillators in zero gravity.	No apparent effect of heat flux. Continuous growth in both normal and zero gravities.
Coalescence	Small amount at low heat flux in normal and zero gravities. An increase with increasing heat flux in normal gravity. A considerable increase with increasing heat flux in zero gravity.	Little noticeable at low heat flux in either normal or zero gravity. No change with increasing heat flux in normal gravity. Slight increase with increasing heat flux in zero gravity.
Bubble population	An increase with increasing heat flux in normal and zero gravities. No apparent effect of gravity.	An increase with increasing heat flux in normal and zero gravities. Greater than at low subcooling away from inception point. No apparent effect of gravity.
Bubble maximum radii	No apparent effect of heat flux or gravity at low heat flux.	No apparent effect of heat flux or gravity. Smaller than at low subcooling.
Bubble lifetime	No apparent effect of heat flux or gravity at low heat flux.	No apparent effect of heat flux or gravity. Smaller than at low subcooling.

DISCUSSION OF GRAVITY EFFECTS ON BUBBLE DYNAMICS

Bubble Characteristics

The primary purpose of the work of the authors has been to determine the effect of gravity on boiling under conditions in which the formation and departure of individual bubbles on a heated surface dominates the heat-transfer mechanism. Therefore, one of the characteristics studied statistically was the maximum radii bubbles attain while they are attached to the surface. This investigation was conducted for a range of subcoolings and heat-transfer rates and for various fluid properties.

The effects of gravity on bubble characteristics at various subcoolings were investi-

gated with water. At higher subcoolings tested ($T_{sat} - T_{bulk} \geqq 35^O$ F; 19.45^O K), little difference was evident between the normal- and zero-gravity results, as shown in figure 6(a). However, for the lower subcoolings tested ($T_{sat} - T_{bulk} \leqq 10^O$ F; 5.56^O K), there was a trend to larger bubbles in zero gravity than in normal gravity. In fact, for the lowest subcooling tested ($T_{sat} - T_{bulk} \cong 5^O$ F; 2.78^O K) in zero gravity, it appeared that a transition out of the discrete bubble region had occurred because of the considerable amount of coalescence and agglomeration about the heater surface.

The effects of a reduction in surface tension on bubble maximum radius were investigated by testing a liquid (an ethanol-water solution) with a surface tension approximately 30 percent that of water over a range of subcoolings in normal and zero gravities. The density and viscosity of this solution were approximately the same as those for water. The results, along with those for water, are shown in figure 6(b). It is evident that a reduction in surface tension from that of water resulted in little difference between the normal- and zero-gravity bubble characteristics.

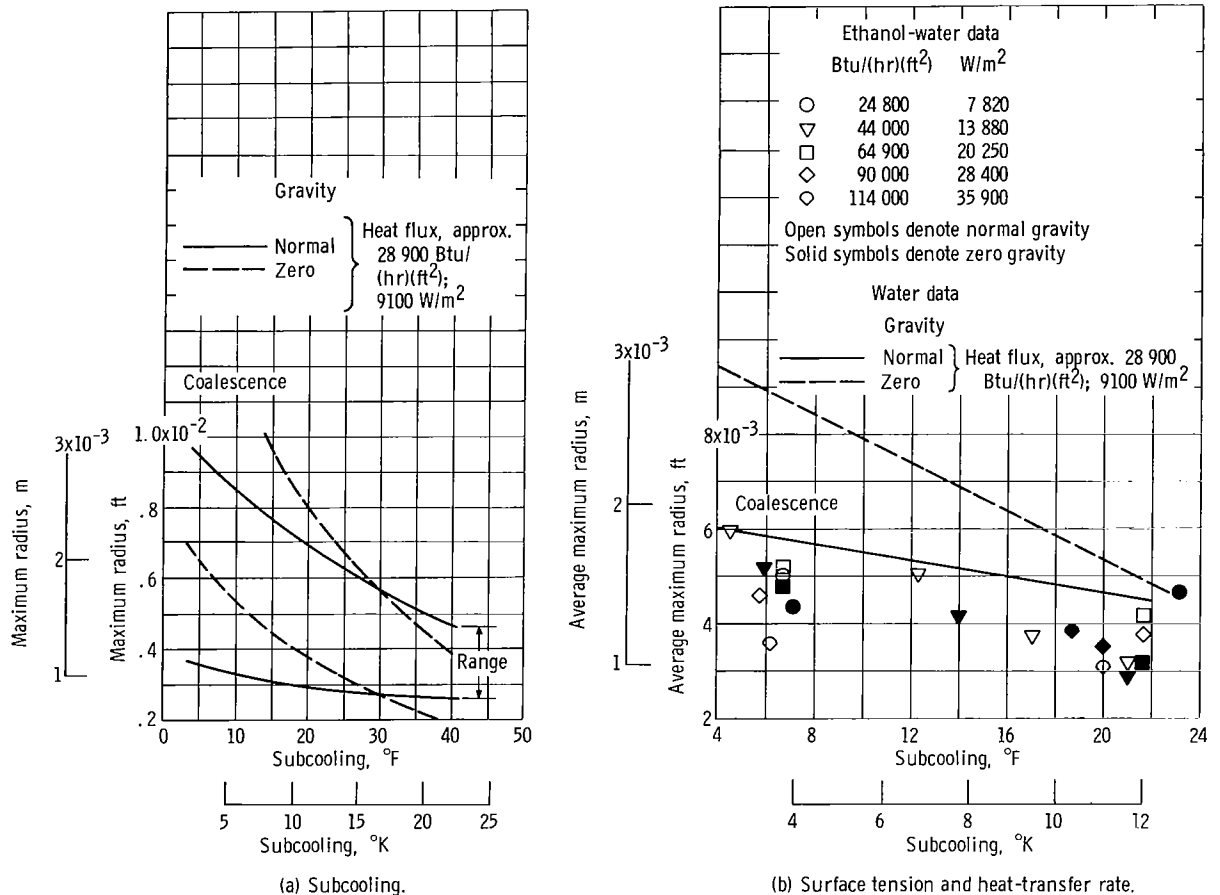The effect of heat-transfer rate at various subcoolings in normal and zero gravities

(a) Subcooling.

(b) Surface tension and heat-transfer rate.

Figure 6. – Effects of gravity on bubble maximum radius as function of subcooling, surface tension, and heat-transfer rate. Experimental data from reference 7.

for the ethanol-water solution is also indicated in figure 6(b). No effect of gravity as a function of heat-transfer rate at low heat fluxes is evident. However, no data are presented for the higher heat-transfer rates at the lower subcooling tested ($T_{sat} - T_{bulk} \cong 6^O$ F; 3.34^O K) in zero gravity. The predominance of coalescence due to (1) the relatively high population density and (2) the fact that bubbles lingered in the vicinity of the surface after separation suggests that a transition out of the discrete bubble region had occurred.

Another characteristic which was investigated statistically was bubble lifetime, or the time a bubble remained attached to the surface. The results of the effect of gravity as a function of subcooling, surface tension, and heat-transfer rate on bubble lifetime, as shown in figure 7, were similar to the findings of the maximum-radii study.
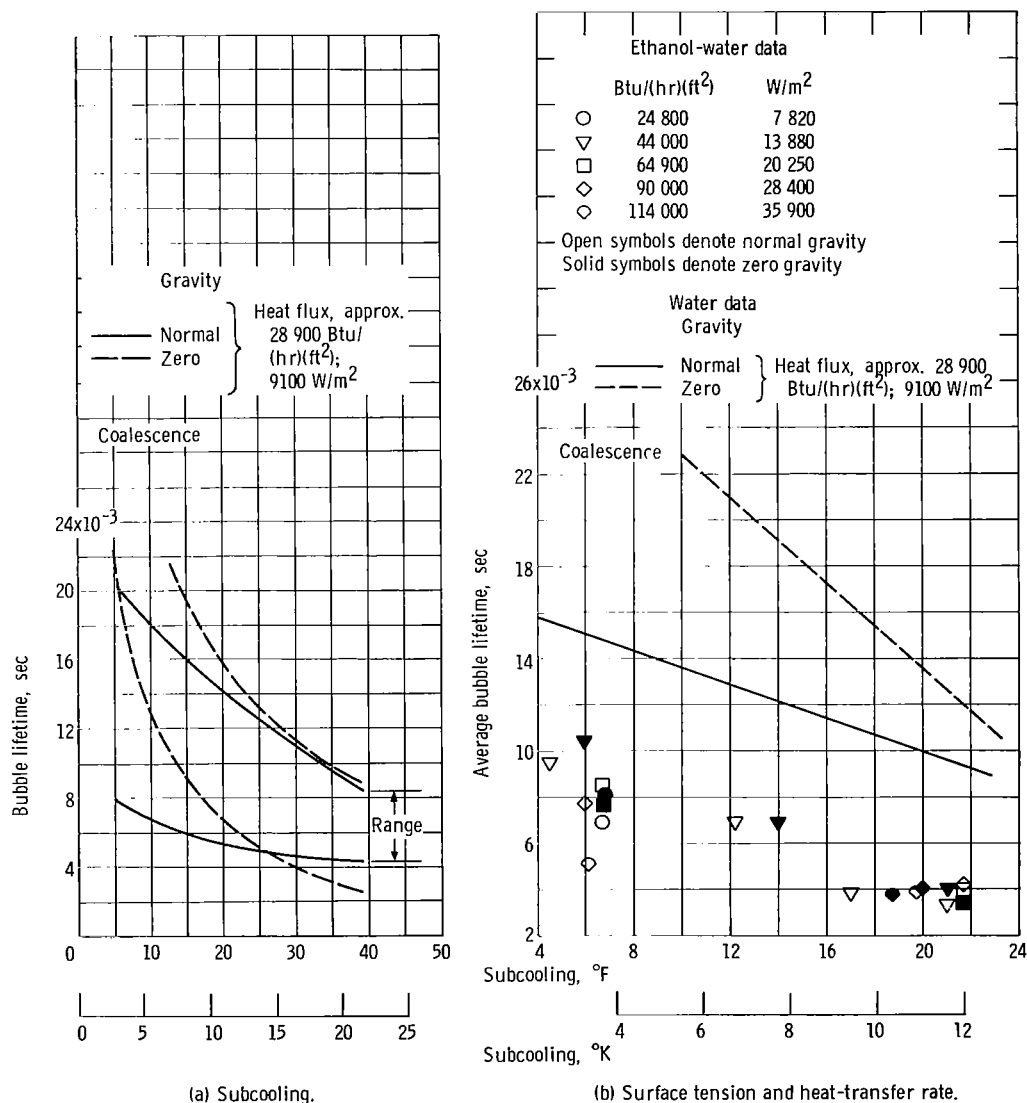

(a) Subcooling.   (b) Surface tension and heat-transfer rate.

Figure 7. – Effects of gravity on bubble lifetime as function of subcooling, surface tension, and heat transfer rate. Experimental data from reference 7.

The statistical data suggest that gravity independent boiling occurred for the higher subcoolings with all the test liquids and for all subcoolings at the lower heat-transfer rates with the ethanol-water solution. However, before positive conclusions can be drawn, a detailed study of the forces acting on the bubbles is necessary in order to determine the importance of gravity on the dynamics of the bubbles.

Discussion of Forces

The force analysis, as presented earlier in this report, was applied to average bubbles for the tests in which subcooling, surface tension, and viscosity were varied. An average bubble was defined as one whose maximum-radii and lifetime characteristics were as close to the statistical average as possible. Force histories, plots of force against time, were prepared for the individual bubbles so that the stimulus for removal could be studied.

Effects of gravity for different subcoolings. - Force histories for water are presented in figure 8 for the higher and lower subcoolings tested in normal and zero gravities. It is apparent that, at the low-subcooling - normal-gravity test condition, buoy-

(a) High subcooling ($T_{sat} - T_{bulk} \cong 35°$ F; 19.4 °K).

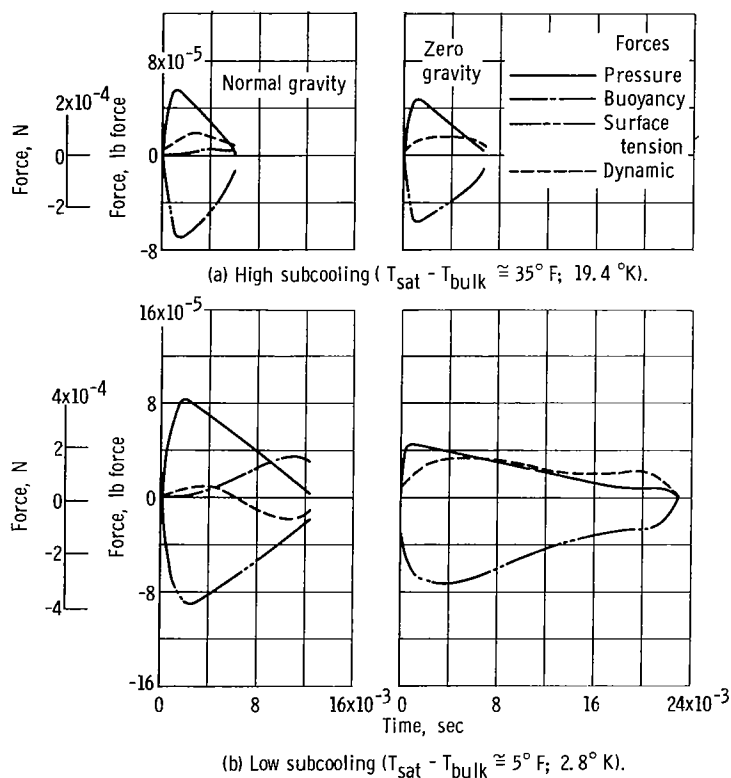(b) Low subcooling ($T_{sat} - T_{bulk} \cong 5°$ F; 2.8° K).

Figure 8. - Dynamics of water bubbles at high and low subcoolings in normal and zero gravities.

ancy had a relatively large role in determining the motion of the bubbles. Therefore, at a comparable subcooling in zero gravity, the dynamics of the bubbles would be expected to be altered because of the absence of the buoyant force. As shown in figure 8, the normal- and zero-gravity force histories were significantly different, which indicated the gravity dependence of bubble dynamics at this test condition. However, the bubbles still separated from the surface in zero gravity because of an increase in the dynamic force. In contrast, at high subcooling, the unimportance of the buoyant force in normal gravity accounts for the similar normal- and zero-gravity histories. Therefore, from this force data and the statistical results, it may be concluded that boiling is independent of gravity at higher subcoolings.

Effects of gravity for different viscosities. - A liquid which had a viscosity approximately 10 times that of water, that is, a 60-percent sugar-water solution was selected in order to investigate the effects of gravity at different viscosities. The surface tension and density of this solution was approximately the same as that for water. The bubble lifetime and maximum-radii statistical data for this liquid were not presented earlier because the trends regarding its gravity dependence at the different subcoolings were the same as those for water. However, dynamic effects caused by the difference in viscosity are apparent from the force histories, as shown in figure 9. For water, the drag
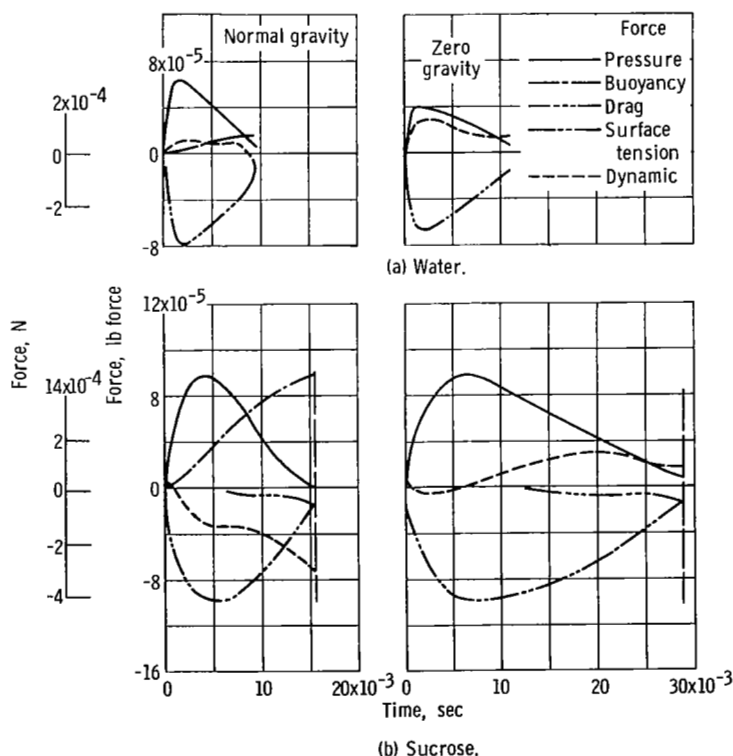

Figure 9. - Dynamics of bubbles generated in liquids of different viscosities at approximately 15° F (8.3° K) subcooling in normal and zero gravities. Experimental data from reference 8.

force was so small that it was not plotted. Also in this figure, the sucrose force histories indicate that, although in normal gravity the drag was small in relation to the buoyancy and dynamic forces, in zero gravity near separation the drag force had a value comparable to the other forces and must have been of importance in determining the resultant motion of the bubble.

Effects of gravity for different surface tensions. - The bubble-lifetime and maximum-radii statistical analysis indicated that for the ethanol-water solution similar characteristics were obtained in normal and zero gravities at comparable subcoolings. At higher subcoolings, this similarity is readily explained by the small role of the buoyancy force in normal gravity. However, as shown in figure 10, which presents force histories as
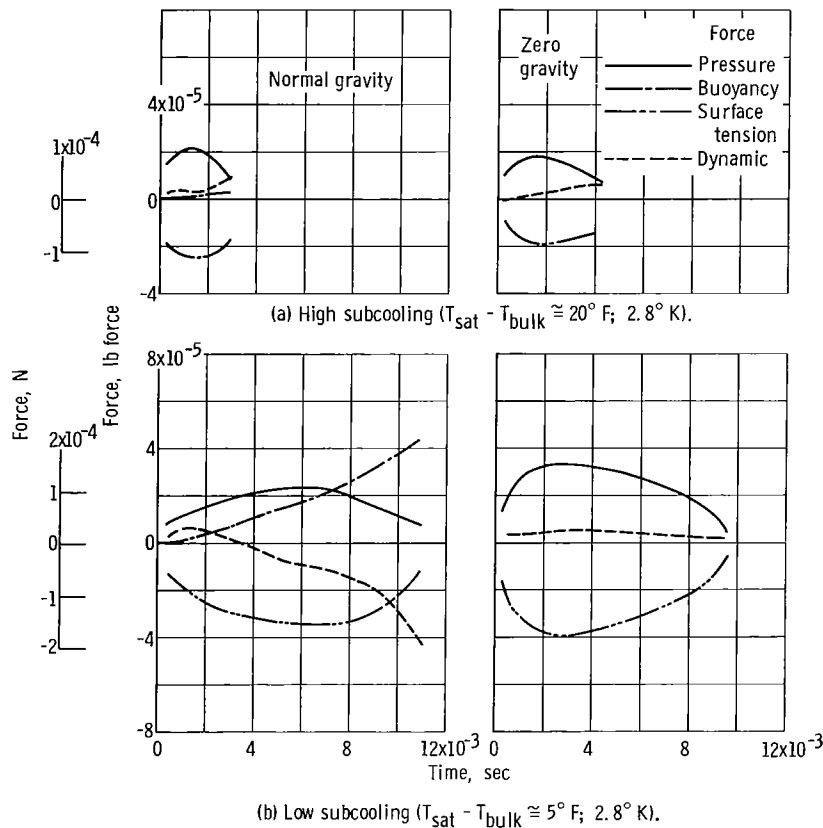

(a) High subcooling ($T_{sat} - T_{bulk} \cong 20°$ F; 2.8° K).

(b) Low subcooling ($T_{sat} - T_{bulk} \cong 5°$ F; 2.8° K).

Figure 10. - Dynamics of bubbles generated in liquid of reduced surface compared to water at low and high subcoolings in normal and zero gravities. Experimental data from reference 8.

a function of subcooling and gravity level, at lower subcooling, there is a great difference between the normal- and zero-gravity histories. Apparently, at low subcooling, geometric or dynamic changes took place in zero gravity, in addition to the effective absence of gravity, to enable the bubbles to separate from the surface with approximately the same average maximum radius and lifetime as was observed for normal gravity.

A difference that was evident between the water and ethanol-water bubbles was that bubbles generated in the ethanol-water solution were more spherical. A measure of the distortion of the bubbles from spherical may be obtained from the ratio of the absolute magnitude of the pressure force to the surface-tension force. For a perfect sphere, the value of this quantity is 1. This ratio also reflects the relative importance of the pressure force as a removal agent. A plot of this distortion parameter against dimensionless time (the ratio of real time to bubble lifetime) in figure 11 indicates the more spherical
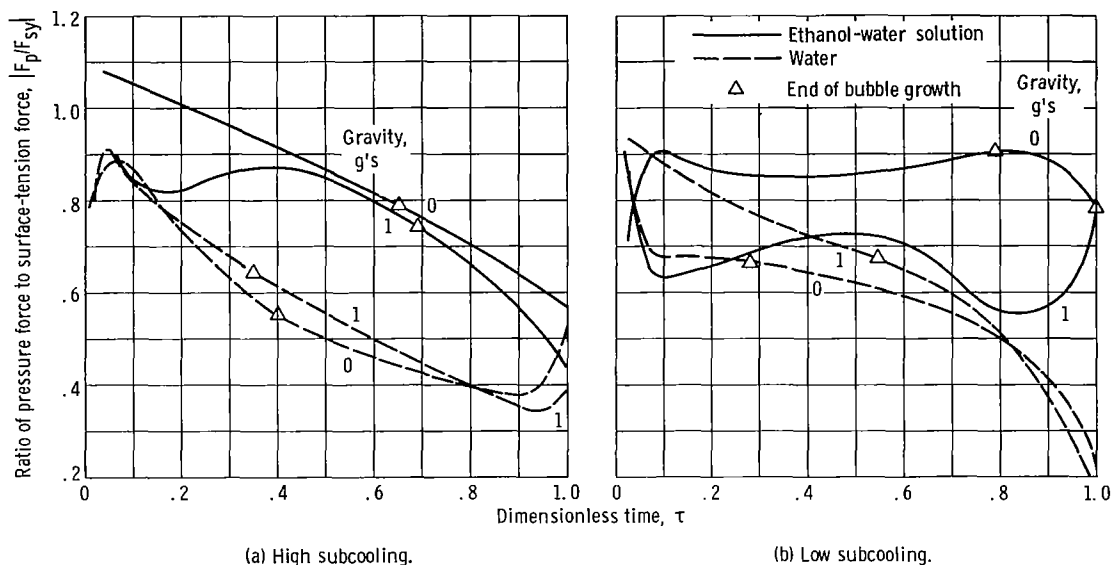

(a) High subcooling.   (b) Low subcooling.

Figure 11. – Distortion of bubbles from spherical at high and low subcoolings.

nature of the ethanol-water bubbles as compared to those generated in water. It is also apparent that, at lower subcooling, the ethanol-water bubbles in zero gravity were more spherical than bubbles generated in the same liquid in normal gravity. Therefore, the pressure force dominated the removal effects for this liquid at higher subcooling in both gravity levels and at lower subcooling in zero gravity, as shown in figure 10.

Effects of gravity for different heat-transfer rates. - In the section Effects of Heat-Transfer Rate on Bubble Dynamics, the lifetime and maximum radii of ethanol-water bubbles generated over a range of heat fluxes is presented. It was shown that, for these test conditions, there was no effect of gravity on the bubble characteristics investigated (see fig. 4). Because the relative importance of the different forces acting on bubbles generated in an ethanol-water solution is presented in a previous report (ref. 8) for one heat flux (44 200 Btu/(hr)(ft^2); 13 900 W/m^2), and because the bubble growth characteristics did not change with gravity or heat flux in the discrete bubble region, the force analysis was not performed for different heat fluxes.

SUMMARY OF RESULTS

An experimental study of the effects of gravity on boiling bubble dynamics from a flat horizontal surface and in the heat flux range defined as the discrete bubble region for various subcoolings ($T_{sat} \simeq T_{bulk} = 5^O$ to 40° F; 2.78^O to 22.22^O K), fluid properties, and heat-transfer rates (24 800 to 114 000 Btu/(hr)(ft^2); 7820 to 35 900 W/m^2) yielded the following results:

1. An increase in subcooling resulted in the dynamics of bubbles becoming gravity independent.

2. An increase in viscosity to 10 times that of water resulted in drag on the bubbles becoming of more importance near separation in a zero-gravity environment.

3. A reduction in surface tension to one-third that of water resulted in the normal- and zero-gravity average maximum-radii and lifetime characteristics of these bubbles becoming similar.

4. A variation of heat flux within the discrete bubble region has no effect as a function of gravity on the average maximum radii and lifetime of bubbles generated in an ethanol-water solution. A significant effect was that, at the lower subcooling tested, the transition from the discrete bubble region occurred at a lower heat flux in zero gravity than in normal gravity.

Additional findings concerning boiling in general are as follows:

5. The newly defined pressure force was of significance in determining the motion of a generated bubble.

6. Viscous effects on a bubble were negligible during its growth.

7. Away from the inception point of boiling, the population density of bubbles tended to be greater at higher subcoolings than lower subcoolings for a particular heat-transfer rate.

Lewis Research Center,
  National Aeronautics and Space Administration,
    Cleveland, Ohio, August 8, 1967,
      124-09-03-01-22.

REFERENCES

1. Aydelott, John C.: Normal Gravity Self-Pressurization of 9-Inch- (23 Cm) Diameter Spherical Liquid Hydrogen Tankage. NASA TN D-4171, 1967.

2. Siegel, R.; and Usiskin, C.: A Photographic Study of Boiling in the Absence of Gravity. J. Heat Transfer, vol. 81, no. 3, Aug. 1959, pp. 230-236.

3. Usiskin, C. M.; and Siegel, R.: An Experimental Study of Boiling in Reduced and Zero Gravity Fields. J. Heat Transfer, vol. 83, no. 3, Aug. 1961, pp. 243-253.

4. Siegel, R.; and Keshock, E. G.: Effects of Reduced Gravity on Nucleate Boiling Bubble Dynamics in Saturated Water. A.I.Ch.E. J., vol. 10, no. 4, July 1964, pp. 509-517.

5. Keshock, Edward G.; and Siegel, Robert: Forces Acting on Bubbles in Nucleate Boiling Under Normal and Reduced Gravity Conditions. NASA TN D-2299, 1964.

6. Siegel, Robert; and Keshock, Edward G.: Nucleate and Film Boiling in Reduced Gravity From Horizontal and Vertical Wires. NASA TR R-216, 1965.

7. Cochran, Thomas H.; and Aydelott, John C.: Effects of Subcooling and Gravity Level on Boiling in the Discrete Bubble Region. NASA TN D-3449, 1966.

8. Cochran, Thomas H.; and Aydelott, John C.: Effects of Fluid Properties and Gravity Level on Boiling in the Discrete Bubble Region. NASA TN D-4070, 1967.

9. Gaertner, R. F.: Photographic Study of Nucleate Pool Boiling on a Horizontal Surface. J. Heat Transfer, vol. 87, no. 1, Feb. 1965, pp. 17-29.

10. Gaertner, R. F.: Distribution of Active Sites in the Nucleate Boiling of Liquids. Chem. Eng. Progr. Symp. Ser., vol. 59, no. 41, 1963, pp. 52-61.

11. Hatton, A. P.; and Hall, I. S.: Photographic Study of Boiling on Prepared Surfaces. Proceedings of the Third International Heat Transfer Conference, Chicago, Aug. 7-12, 1966, A.I.Ch.E.-ASME, 1966, vol. 4, pp. 24-37.